Published in final edited form as:

Nat Cell Biol. ; 13(8): 952–957. doi:10.1038/ncb2291.

Cytoskeletal polarity mediates localized induction of the heart progenitor lineage

James Cooley[1], **Stacia Whitaker**[1], **Sarah Sweeney**[1,2], **Scott Fraser**[2], and **Brad Davidson**[1]

[1] Department of Molecular and Cellular Biology, Molecular Cardiovascular Research Program, University of Arizona, AZ 85724

[2] Department of Biology, Imaging Center, Beckman Institute, California Institute of Technology, CA 91125

Abstract

Cells must make appropriate fate decisions within a complex and dynamic environment [1]. *in vitro* studies suggest that the cytoskeleton acts as an integrative platform for this environmental input[2]. External signals regulate cytoskeletal dynamics and the cytoskeleton reciprocally modulates signal transduction[3, 4]. However, *in vivo* studies linking cytoskeleton/signaling interactions to embryonic cell fate specification remain limited[5-7]. Here we show that the cytoskeleton modulates heart progenitor cell fate. Our studies focus on differential induction of heart fate in the basal chordate *Ciona intestinalis*. We have found that differential induction does not simply reflect differential exposure to the inductive signal. Instead, pre-cardiac cells employ polarized, invasive protrusions to localize their response to an ungraded signal. Through targeted manipulation of the cytoskeletal regulator CDC42, we are able to de-polarize protrusive activity and generate uniform heart progenitor fate specification. Furthermore, we are able to restore differential induction by re-polarizing protrusive activity. These findings illustrate how bi-directional interactions between intercellular signaling and the cytoskeleton can influence embryonic development. In particular, these studies highlight the potential for dynamic cytoskeletal changes to refine cell fate specification in response to crude signal gradients.

A core set of inductive signals guide multiple embryonic cell fate decisions. For example, fibroblast growth factor (FGF) signaling impacts the fate of heart, liver, brain, and numerous other progenitor lineages[8, 9]. FGF and other inductive cues must be processed with high fidelity, as alterations in progenitor numbers can disrupt organ size and function[10]. However, labile embryonic cell interactions generate a high degree of signaling noise[1]. *in vitro* studies indicate that the cytoskeleton helps refine the response of cells to fluctuating micro-environments[2]. Although evidence is accumulating for similar processes in vivo, potential cytoskeletal contributions to FGF signaling or heart progenitor specification have not been investigated.

Correspondence should be addressed to B.D. (bjd18@email.arizona.edu).

Low cell numbers, fixed lineages and rapid development make *Ciona* embryos a powerful model for *in vivo* analysis of cell signaling and fate specification[11-13]. The *Ciona* heart lineage can be traced back to four pre-cardiac "founder" cells in the gastrulating embryo (two symmetrical pairs, each consisting of a B8.9 and B8.10 blastomere, Fig. 1a,a′). During neurulation (stage 15) the founder cells divide asymmetrically, producing unequally sized daughter cells with distinct fates (Fig. 1d-e′). The smaller daughters give rise to the heart progenitor lineage (hp or trunk ventral cells) while their larger sisters give rise to anterior tail muscle precursors (atm). Previous research indicates that heart progenitor induction involves activation of MAP Kinase (MAPK) by fibroblast growth factor 9/16/20 (FGF9)[14, 15]. However, previous work did not address how FGF9 differentially induces heart fate in the smaller daughter cells and not in their sister lineage.

We initiated our investigation into differential heart progenitor induction by examining the precise *in vivo* relationship between the *FGF9* expression domain and labeled founder cells (Fig. 1a-d and S1). These assays indicate that founder cells are first exposed to high levels of FGF9 during gastrulation (stage 13) when *FGF9* is up-regulated in the adjacent mesenchyme and tail muscle lineages (Fig. 1a vs. b, S1a vs. b). At this stage, both founder cells (B8.9 and B8.10) are surrounded by *FGF9* expressing cells (Fig. S1b). This pattern persists as each founder cell divides to produce a smaller anterior-ventral heart progenitor and a larger posterior-dorsal daughter (Fig. 1c-e, S1c-d). FGF9 antibody staining confirms that FGF9 producing cells are positioned all along the division axis of neighboring mitotic founder cells (Fig. S1e-f). Thus it appears that differential induction does not reflect differential exposure to the inductive ligand.

We validated this interpretation of our FGF9 expression assays through dissociation of transgenic Mesp-GFP, FoxF-RFP embryos (Fig. 1f-j, S2). In these assays Mesp-GFP marks the founder cell lineage while FoxF-RFP serves as a read out for FGF/MAPK induction[14]. Although staggered development of founder cells both within and between embryos complicated this dataset (Fig. S1, S2, Movie S4), the overall trends were clear. Individual founder lineage cells dissociated between stages 10-12 produce FoxF-RFP negative clone pairs, indicating the absence of prior induction (Fig. 1f). At stage 13, levels of induction increased significantly (Fig. 1g,j). Strikingly, founder cells isolated at stage 13 undergo uniform induction, generating homogeneous pairs of FoxF-RFP positive daughters (Fig. 1g, 97/115 induced pairs). A significant rise in the prevalence of heterogeneous FoxF-RFP expression, indicative of differential induction, occurs in founder cell clones dissociated shortly before asymmetric division (stage 14, Fig. 1h,i and S2d, n=264, p=0.004). These results suggest that initial exposure to FGF9 results in uniform receptor occupancy. Furthermore, it appears that an extrinsic cue present only in intact embryos localizes inductive signaling shortly before asymmetric division.

We next examined the morphology of mitotic founder cells. Just prior to division (stage 14), founder cells exhibit a striking, highly polarized enrichment of protrusions (Fig. 2a-b, S3b, Movies S1-2). This protrusive fringe is concentrated along the anterior-ventral edge of founder cell pairs (asterisks in Fig. 2a′b′, Movies S1,2); the region where heart progenitor daughter cells will shortly emerge (Fig. 2c, Movie S3). Remarkably, the founder cell protrusive fringe penetrates the underlying ventral epidermis, sometimes forming an

invasive membrane that outlines the basal-lateral surfaces of neighboring epidermal cells (Fig. 2b, Movie S2). Through time-lapse imaging we observed the formation of large anterior-ventral founder cell protrusions within living embryos (Movies S4-6). Founder cell protrusions are highly invasive, reaching deep into the underlying epidermis (Movie S4). These protrusions are transient structures forming just prior to founder cell division and terminating shortly after division is complete (Movie S4-6). Thus, protrusive activity (stage 14/15) does not correlate temporally with initiation of heart progenitor migration (stage 18). In summary, we have found that the founder cell cortex is highly polarized, generating invasive protrusions at the site of differential induction.

The observed correlation between protrusions and localized induction may reflect an instructive role for cortical actin in regional FGF signaling[16, 17]. To explore this hypothesis, we assayed FGF receptor activation using a phospho-Tyrosine (pTyr) antibody. We simultaneously visualized filamentous actin (f-actin) in founder cells through targeted expression of the actin binding fusion protein Utrophin-GFP[18] (Fig. 2d-f). Regional enrichment of f-actin along the founder cell cortex was consistently associated with regional enrichment of p-Tyr staining in the adjacent membrane (Fig. 2d-f). At stage 13, founder cells display uniform, ventral enrichment of f-actin mirroring un-polarized protrusions along this surface (Fig. 2d and Fig. S3a). p-Tyr staining in the adjacent ventral membrane was also un-polarized (Fig. 2d, quantified in 2h). Beginning at stage 14, f-actin and p-Tyr staining become concentrated at the anterior-ventral edge (Fig. 2e, h) mirroring the emergence of the protrusive fringe at this stage (Fig. 2a and S3b). This cytoskeletal/signaling polarity persists after division, with the smaller anterior-ventral heart progenitor daughter cells displaying distinctly higher levels of Utr-GFP and p-Tyr staining in comparison with their larger posterior-dorsal sisters (Fig. 2f). Thus, as founder cells prepare to divide, it appears that cortical f-actin and FGF receptor activation are gradually localized to the presumptive heart progenitor membrane (Fig. 2g). We verified that polarized p-Tyr staining reflects polarized FGF receptor activation through targeted expression of a previously characterized dominant negative FGF receptor (Mesp-FGFRdn[14]). This manipulation reduced p-Tyr staining in the founder cells and eliminated anterior-ventral enrichment (Fig. 2h). The polarization of inductive signaling between stages 13 and 14 correlates with the shift from uniform induction to differential induction observed in founder cells isolated at these stages (Fig. 1g-i, S2). These results indicate that FGF receptor activation is locally enhanced in association with polarized protrusive activity.

Localized activation of the Rho GTPase, CDC42, often directs polarized actin dynamics[19, 20]. We therefore examined CDC42 activation in stage 14 founder cells using a FRET based CDC42 activation bio-probe[21] (Fig. 3a,b). The bioprobe revealed a modest but significant polarization of CDC42 activation along the AV-PV axis while an inactive control probe showed no polarization (Fig. 3b). These assays indicate that CDC42 activation is significantly enriched on the anterior-ventral side, the site of enhanced protrusion and subsequent differential induction.

Our correlative data suggests a functional role for localized CDC42 activity in induction. To test this hypothesis, we disrupted localized CDC42 activity by expressing constitutively active CDC42 in the heart founder cell lineage (Mesp-Cdc42 Q61L)[22]. While targeted

expression of full length CDC42 had no discernible impact (Fig. 3g, 4a,d and S3b), targeted expression of the GTPase defective Q61L mutant generated uniform protrusive activity (Fig. S3c) and uniform ventral phospho-Tyrosine staining (Fig. 4d), indicating depolarization of FGF receptor activation. Most significantly, Mesp-Cdc42 Q61L disrupted differential induction (Fig. 3d, 4b). In the majority of Mesp-Cdc42 Q61L embryos, FoxF reporter (Fig. 3g) and heart marker gene expression (*FoxF*, *Hand-like* and *GATA-a*, Fig. S4) were expanded and often encompassed all founder lineage cells. Additional experiments demonstrate that Cdc42 Q61L potentiates induction through the FGF/MAPK pathway (Fig. S5).

Intriguingly, targeted expression of a different constitutively active CDC42 construct, the fast cycling mutant F28L (Mesp-Cdc42 F28L), did not have any discernable impact on founder cell induction (Fig. 3e,g). We therefore hypothesized that localized CDC42 activity requires sustained association with the anterior-ventral plasma membrane. According to this model, periodic membrane release/inactivation of the fast cycling mutant would prevent it from generating ectopic CDC42 activity. In contrast, sustained and unlocalized membrane association allows the Q61L mutant to generate uniform CDC42 activity. We tested this hypothesis by mutating the Rho insert domain in the Cdc42 F28L construct (Mesp-Cdc42 F28L-ΔRho). Previous studies have shown that the Rho insert can facilitate removal of CDC42 from the membrane and subsequent inactivation in the cytosol[23, 24]. As predicted by our model, targeted expression of the fast-cycling Rho deletion mutant (Mesp-Cdc42 F28L-ΔRho) generated significant levels of uniform induction while targeted expression of a wild-type Rho deletion mutant (Mesp-Cdc42ΔRho) had no effect (Fig. 3f,g). These results demonstrate that disruptions of differential induction by activated CDC42 constructs are not merely an artifact of hyperactive CDC42. Instead, our manipulations of CDC42 strongly support a model in which polarized activation of CDC42 at the anterior-ventral membrane promotes regional enrichment of inductive signaling.

We next examined CDC42 localization through targeted expression of Cdc42-GFP fusion proteins (Mesp-Cdc42-GFP, Mesp-Cdc42 Q61L-GFP, Mesp-Cdc42 F28L-GFP and Mesp-Cdc42 F28L-ΔRho-GFP, Fig. 3h-i, S3f-g). By co-staining with anti-tubulin antibodies, we were able to visualize CDC42 localization during discrete cell cycle phases and precisely identify the presumptive heart progenitor membrane in mitotic founder cells. We found that Cdc42-GFP and Cdc42 F28L-GFP were strongly enriched along the presumptive heart progenitor membranes of dividing founder cell pairs (Fig. 3h-i, S3f). In contrast, Cdc42 Q61L-GFP and Cdc42 F28L-ΔRho-GFP were expressed in a more diffuse, uniform pattern (Fig. 3h, S3g). Thus, as predicted by our model, it appears that disruption of polarized CDC42 activation along the founder cell membrane is required to disrupt regional signaling (compare Fig. 3g to 3h). Taken together with our data on localized protrusions (Fig. 2), these results suggest that polarized CDC42 impacts regional induction through regulation of cytoskeletal dynamics.

We next focused on determining whether localized actin dynamics mediate the impact of polarized CDC42 on inductive signaling (Fig. 4 and S6). To generate protrusions, CDC42 often works in tandem with Rac to activate the actin nucleator Arp2/3[25]. We therefore anticipated that expression of constitutively active Rac would disrupt differential induction.

As predicted, targeted expression of active Rac (Mesp-RacG12V[26, 27]) potentiated uniform induction (p=2.5E-03, Fig. S6c). We also anticipated that interference with Arp2/3 function would disrupt differential induction. We therefore treated embryos with the Arp2/3 inhibitor Ck-666[28] during the period of founder cell polarization (stages 12-14). As predicted, this treatment disrupted localized enhancement of founder cell p-Tyr staining and potentiated uniform induction (p=9.8E-03, Fig. S6a-d). However, whole embryo disruption of actin nucleation is likely to have numerous indirect effects on development that may impact induction. We therefore attempted to specifically interfere with CDC42 mediated actin nucleation in the founder cell lineage. Wasp functions downstream of CDC42 to promote ARP2/3 mediated nucleation of actin in filopodia and invadopodia[19, 20]. We constructed a truncated form of *Ciona* Wasp (WaspΔVCA) in which the C-terminal ARP2/3 and actin binding domains are removed, while the N-terminal WH1, PRB, CDC42 binding domain (CRIB) and a single verprolin actin binding domain remain intact. Previous studies have demonstrated that WaspΔVCA specifically disrupts CDC42 mediated activation of endogenous Wasp[29]. Targeted expression of WaspΔVCA (Mesp-WaspΔVCA) appeared to reduce but not fully disrupt the polarity of founder cell protrusions (Fig. S3e). Accordingly, this manipulation reduced but did not eliminate polarized phospho-Tyrosine staining (Fig. 4d) and had no significant impact on differential induction ($p > 0.5$). We then co-transfected embryos with Mesp-WaspΔVCA and Mesp-Cdc42 Q61L. In these embryos, disruption of the Wasp/CDC42 interaction rescues the localization of founder cell protrusions (compare Fig. S3c vs. d) and restores polarized tyrosine phosphorylation (Fig. 4d). Remarkably, co-transfection with WaspΔVCA also led to a significant restoration of differential induction in the Cdc42 Q61L transgenic background (Fig. 4c,e). These experiments strongly support a model in which localized protrusions translate polarized CDC42 activity into regional induction (Fig. 4f, Supplemental Discussion). However, the WaspΔVCA construct might act indirectly to inhibit the association of active CDC42 with other effectors. To alleviate this concern we co-transfected embryos with constructs predicted to bind CDC42 without disrupting downstream actin nucleation (full length Wasp and the CDC42 binding domain of Par6, Par6-CRIB). Targeted expression of these control constructs (Mesp-Wasp and Mesp-Par6-CRIB) failed to restore differential induction in the Mesp-Cdc42 Q61L background (Fig. 4e).

This study illustrates how polarized actin dynamics can potentiate localized receptor tyrosine kinase (RTK)/MAPK signaling in the context of uniform receptor occupancy (Fig. 4f, Supplemental Discussion). Previously, the cytoskeleton has been shown to modulate RTK/MAPK signaling during yeast mating, immune synapse formation, oncogenesis, cell migration, and *in vitro* cell fate decisions[2, 4, 17, 30, 31]. Our results indicate that the cytoskeleton also modulates growth factor signaling during *in vivo* specification of embryonic cell types, including the heart lineage.

Our findings in *Ciona* might reflect a conserved role for cytoskeletal dynamics in vertebrate cardiomyocyte specification. Although FGF signaling helps to establish vertebrate cardiomyocyte identity[8], previous studies have not addressed the potential influence of intrinsic mechanical/cytoskeletal properties on cardiomyocyte induction. There are, however, stem cell data implicating cell-matrix interactions in cardiomyocyte

differentiation[32], raising the intriguing possibility that matrix mediated integrin signaling underlies polarization of vertebrate cardiac progenitors cells. Integrin signaling can modulate GTPases and RTK signaling[33] and is closely tied to the formation of invasive membranes[34]. Thus, it will be of great interest to examine whether mechanoregulatory interactions between matrix, integrin and cytoskeleton regulate heart fate in *Ciona* and vertebrate embryos.

This report has critical implications regarding the function of invasive protrusions. Generally, large invasive membranes help anchor cells to neighboring tissues or permit migration through the surrounding matrix[34, 35]. However, dividing *Ciona* founder cells are not engaged in either of these processes. This raises the possibility that invasive membranes can function primarily as signaling regulators; acting like antennae primed for localized signal transduction. This represents a novel perspective on invasive membranes and how they might contribute to a variety of signal-mediated processes, ranging from cancer metastasis to developmental patterning.

Supplementary Material

Refer to Web version on PubMed Central for supplementary material.

Acknowledgments

The Ensconsin-GFP construct was generously provided by F. Robin, the CDC42 constructs by L. Christiaen, the GPI-GFP construct by A. Gregorio and K. Hadjantonakis and the FRET biosensor constructs by M. Matsuda and D. Kamiyama. We would also like to thank G. Rogers and D. Buster for their advice and assistance on antibody production, M. Salanga for guidance on FRET imaging, T. Warholac for assistance with statistical analysis, and M. Barnet for use of his cooling system for live embryo imaging. We thank D. Sherwood, H. Granzier, and A. Wikramanayake along with members of the U. A. Molecular Cardiovascular Research Program for their input and critical evaluation of the manuscript. Live embryo imaging was performed in the facilities of the Biological Imaging Center, under support from the Caltech Beckman Institute and the Beckman Foundation. The work was supported by grants to B.D. from the AHA (0730345N) and NIH (R01HL091027) along with supplemental funding from the American Recovery Act to support J.C. (3R01HL091027-01A1S1) and support for S. W. from the Science Foundation of Arizona.

References

1. Heisenberg CP, Solnica-Krezel L. Back and forth between cell fate specification and movement during vertebrate gastrulation. Curr Opin Genet Dev. 2008; 18:311–316. [PubMed: 18721878]
2. Engler AJ, Sen S, Sweeney HL, Discher DE. Matrix elasticity directs stem cell lineage specification. Cell. 2006; 126:677–689. [PubMed: 16923388]
3. Vicente-Manzanares M, Choi CK, Horwitz AR. Integrins in cell migration--the actin connection. J Cell Sci. 2009; 122:199–206. [PubMed: 19118212]
4. Paszek MJ, et al. Tensional homeostasis and the malignant phenotype. Cancer Cell. 2005; 8:241–254. [PubMed: 16169468]
5. Wozniak MA, Chen CS. Mechanotransduction in development: a growing role for contractility. Nat Rev Mol Cell Biol. 2009; 10:34–43. [PubMed: 19197330]
6. Rajan A, Tien AC, Haueter CM, Schulze KL, Bellen HJ. The Arp2/3 complex and WASp are required for apical trafficking of Delta into microvilli during cell fate specification of sensory organ precursors. Nat Cell Biol. 2009; 11:815–824. [PubMed: 19543274]
7. Desprat N, Supatto W, Pouille PA, Beaurepaire E, Farge E. Tissue deformation modulates twist expression to determine anterior midgut differentiation in Drosophila embryos. Dev Cell. 2008; 15:470–477. [PubMed: 18804441]

8. Srivastava D. Making or breaking the heart: from lineage determination to morphogenesis. Cell. 2006; 126:1037–1048. [PubMed: 16990131]
9. Thisse B, Thisse C. Functions and regulations of fibroblast growth factor signaling during embryonic development. Dev Biol. 2005; 287:390–402. [PubMed: 16216232]
10. Keegan BR, Feldman JL, Begemann G, Ingham PW, Yelon D. Retinoic acid signaling restricts the cardiac progenitor pool. Science. 2005; 307:247–249. [PubMed: 15653502]
11. Satoh N. The ascidian tadpole larva: comparative molecular development and genomics. Nat Rev Genet. 2003; 4:285–295. [PubMed: 12671659]
12. Lemaire P. Unfolding a chordate developmental program, one cell at a time: invariant cell lineages, short-range inductions and evolutionary plasticity in ascidians. Dev Biol. 2009; 332:48–60. [PubMed: 19433085]
13. Munro E, Robin F, Lemaire P. Cellular morphogenesis in ascidians: how to shape a simple tadpole. Curr Opin Genet Dev. 2006
14. Davidson B, Shi W, Beh J, Christiaen L, Levine M. FGF signaling delineates the cardiac progenitor field in the simple chordate, Ciona intestinalis. Genes Dev. 2006; 20:2728–2738. [PubMed: 17015434]
15. Imai KS, Levine M, Satoh N, Satou Y. Regulatory blueprint for a chordate embryo. Science. 2006; 312:1183–1187. [PubMed: 16728634]
16. Sato M, Kornberg TB. FGF is an essential mitogen and chemoattractant for the air sacs of the drosophila tracheal system. Dev Cell. 2002; 3:195–207. [PubMed: 12194851]
17. Lidke DS, Lidke KA, Rieger B, Jovin TM, Arndt-Jovin DJ. Reaching out for signals: filopodia sense EGF and respond by directed retrograde transport of activated receptors. J Cell Biol. 2005; 170:619–626. [PubMed: 16103229]
18. Burkel BM, von Dassow G, Bement WM. Versatile fluorescent probes for actin filaments based on the actin-binding domain of utrophin. Cell Motil Cytoskeleton. 2007; 64:822–832. [PubMed: 17685442]
19. Yamaguchi H, et al. Molecular mechanisms of invadopodium formation: the role of the N-WASP-Arp2/3 complex pathway and cofilin. J Cell Biol. 2005; 168:441–452. [PubMed: 15684033]
20. Etienne-Manneville S. Cdc42--the centre of polarity. J Cell Sci. 2004; 117:1291–1300. [PubMed: 15020669]
21. Kamiyama D, Chiba A. Endogenous activation patterns of Cdc42 GTPase within Drosophila embryos. Science. 2009; 324:1338–1340. [PubMed: 19498173]
22. Miller PJ, Johnson DI. Cdc42p GTPase is involved in controlling polarized cell growth in Schizosaccharomyces pombe. Mol Cell Biol. 1994; 14:1075–1083. [PubMed: 8289788]
23. Wu WJ, Leonard DA, AC R, Manor D. Interaction between Cdc42Hs and RhoGDI is mediated through the Rho insert region. J Biol Chem. 1997; 272:26153–26158. [PubMed: 9334181]
24. Richman TJ, et al. Analysis of cell-cycle specific localization of the Rdi1p RhoGDI and the structural determinants required for Cdc42p membrane localization and clustering at sites of polarized growth. Curr Genet. 2004; 45:339–349. [PubMed: 15108020]
25. Padrick SB, Rosen MK. Physical mechanisms of signal integration by WASP family proteins. Annu Rev Biochem. 79:707–735. [PubMed: 20533885]
26. Heasman SJ, Ridley AJ. Mammalian Rho GTPases: new insights into their functions from in vivo studies. Nat Rev Mol Cell Biol. 2008; 9:690–701. [PubMed: 18719708]
27. Coisy-Quivy M, et al. Identification of Rho GTPases implicated in terminal differentiation of muscle cells in ascidia. Biol Cell. 2006; 98:577–588. [PubMed: 16756514]
28. Nolen BJ, et al. Characterization of two classes of small molecule inhibitors of Arp2/3 complex. Nature. 2009; 460:1031–1034. [PubMed: 19648907]
29. Schafer G, et al. The Wiskott-Aldrich syndrome protein (WASP) is essential for myoblast fusion in Drosophila. Dev Biol. 2007; 304:664–674. [PubMed: 17306790]
30. Yu L, Qi M, Sheff MA, Elion EA. Counteractive control of polarized morphogenesis during mating by mitogen-activated protein kinase Fus3 and G1 cyclin-dependent kinase. Mol Biol Cell. 2008; 19:1739–1752. [PubMed: 18256288]

31. Yuseff MI, Lankar D, Lennon-Dumenil AM. Dynamics of membrane trafficking downstream of B and T cell receptor engagement: impact on immune synapses. Traffic. 2009; 10:629–636. [PubMed: 19416472]

32. Battista S, et al. The effect of matrix composition of 3D constructs on embryonic stem cell differentiation. Biomaterials. 2005; 26:6194–6207. [PubMed: 15921736]

33. Schwartz MA, Ginsberg MH. Networks and crosstalk: integrin signalling spreads. Nat Cell Biol. 2002; 4:E65–68. [PubMed: 11944032]

34. Hagedorn EJ, et al. Integrin acts upstream of netrin signaling to regulate formation of the anchor cell's invasive membrane in C. elegans. Dev Cell. 2009; 17:187–198. [PubMed: 19686680]

35. Linder S. The matrix corroded: podosomes and invadopodia in extracellular matrix degradation. Trends Cell Biol. 2007; 17:107–117. [PubMed: 17275303]

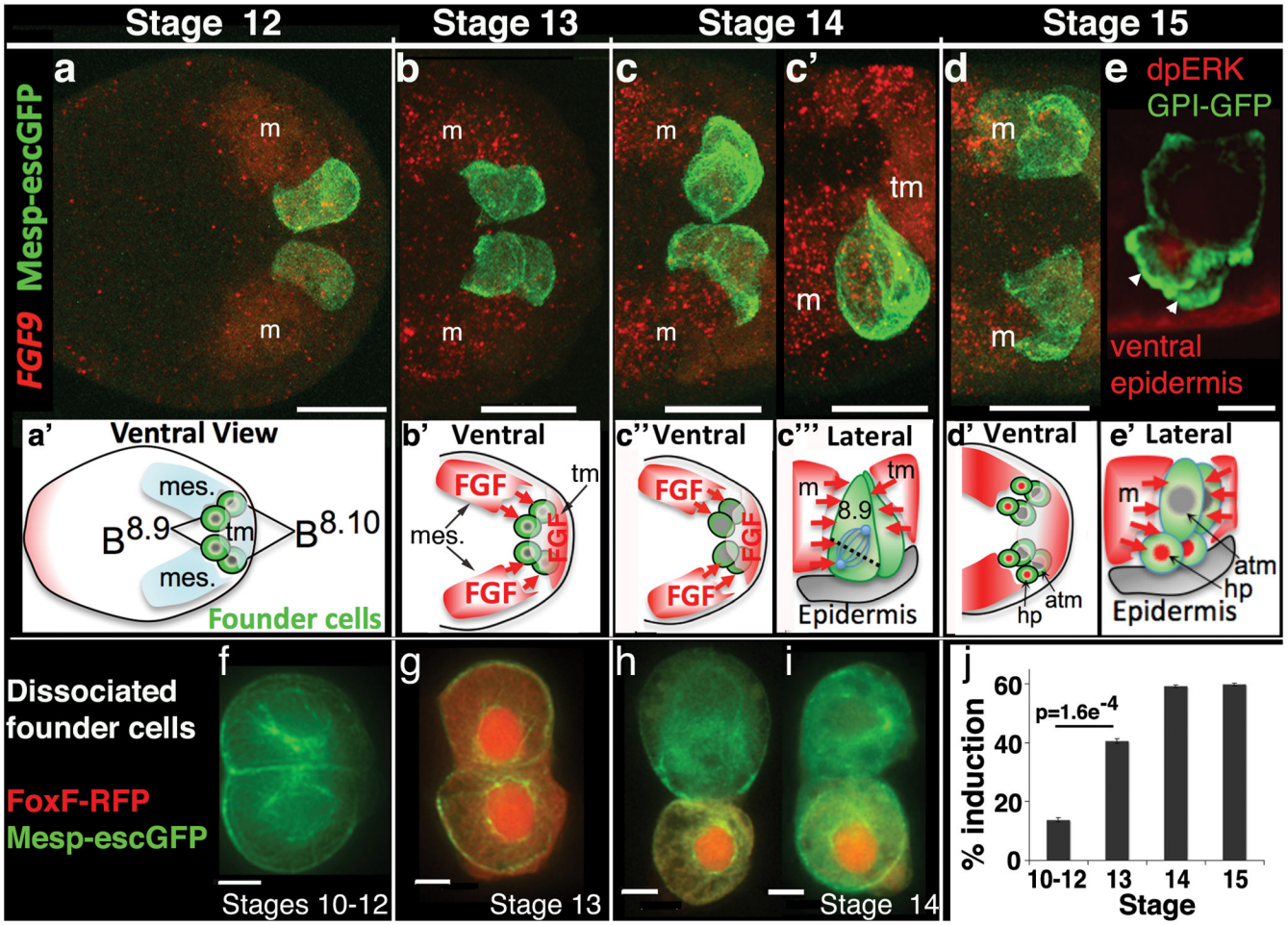

Figure 1. Nature and timing of heart progenitor lineage induction

(**a-d**) Ventral and lateral (**c′**) optical sections of *FGF9 in situ* hybridizations (m = mesenchyme, tm = tail muscle, scale bar = 30μm). (**e**) *In vivo* dpERK antibody staining indicates differential MAPK activation in the smaller heart progenitor cells (arrowheads) shortly after founder cell division, lateral view, scale bar = 10μm. (**a′-e′**) Below each image is a diagram illustrating the spatial relationship between founder cells (B8.9 and 8.10) and *FGF9* expressing cells, (hp = heart progenitor, atm = larger sister cell lineage, mes. or m = mesenchyme). (**f-i**) Representative founder cell clone pairs resulting from staged dissociations, scale bar = 5μm. (**j**) Percent induction (FoxF-RFP positive cells) produced by founder cells isolated at discrete stages, n=1117 for St. 10-12, n=658 for St. 13, n=651 for St. 14 and n=693 for St. 15. Embryos are displayed anterior to the left in these and all subsequent figures.

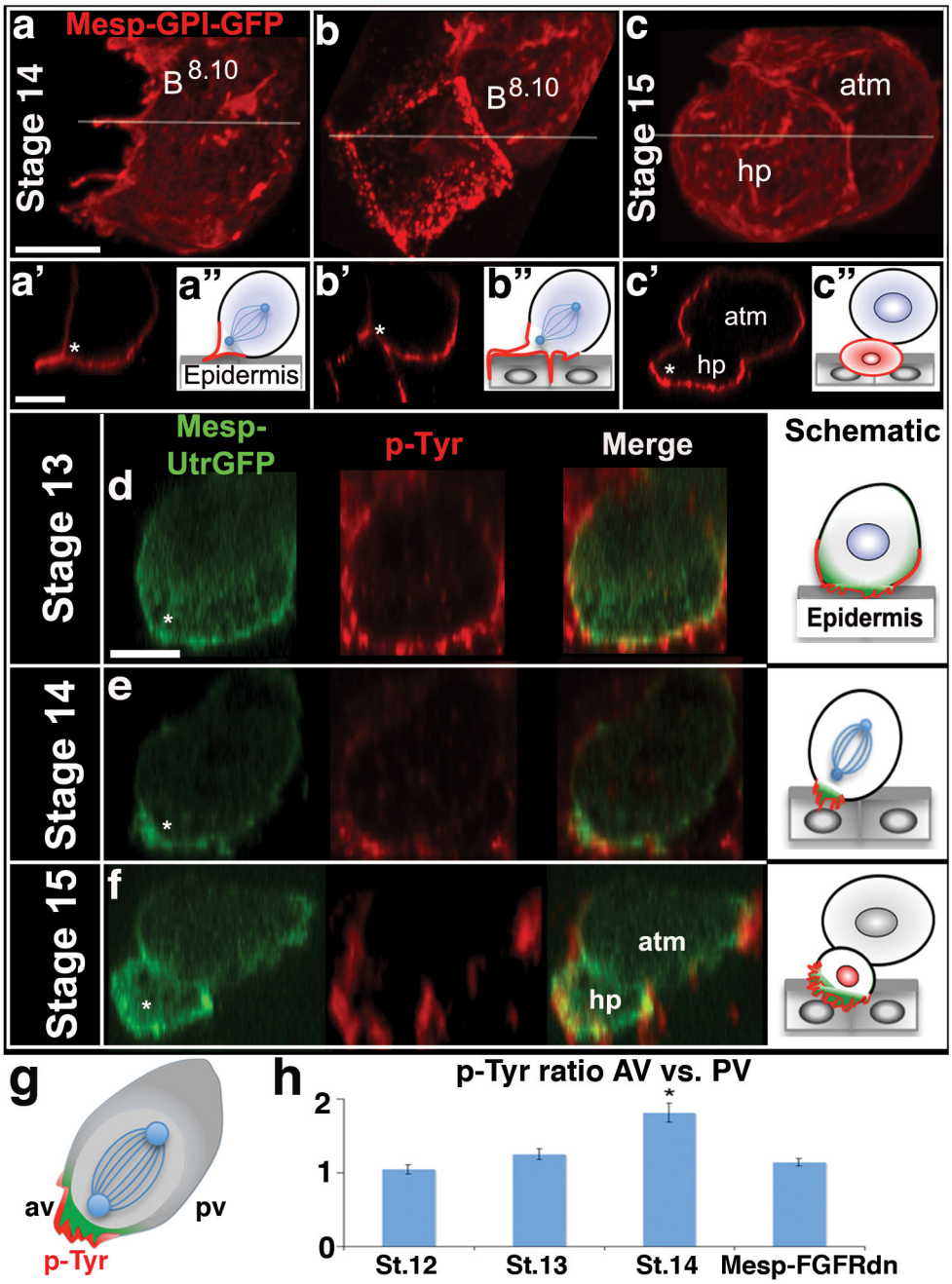

Figure 2. Localized protrusive activity correlates with localized induction

(**a-c**) Ventral projections of membrane anchored-GFP (GPI-GFP) labeled founder lineage cells, Stage 14-15. (**a′-c′**) Lateral optical sections through corresponding stacks at the position indicated in (**a-c**) by white lines. (**a″-c″**) Diagrams illustrating invasion of underlying ventral epidermis. (**d-f**) Representative, lateral optical sections through staged B8.9 founder cells (**d,e**) and their progeny (**f**), green = Utr-GFP and red = pTyr for both images and accompanying schematics. Asterisks indicate the anterior-ventral position at which heart progenitor cells (hp) consistently emerge, atm = anterior tail muscle lineage. (**g**) Schematic of a dividing founder cell (after Fig. 2e) illustrating method for comparing p-Tyr

levels between the anterior-ventral (av) and posterior-ventral (pv) membranes. (**h**) Quantitative analysis of membrane pTyr ratios (AV vs. PV). Note that significant pTyr polarization (asterisk) was first observed at stage 14 (St. 12 p=0.64, n=92; St. 13 p=0.21, n=89; St. 14 p=9.3E-012, n=89) and that this polarization was dependent on FGF signaling (St. 14 Mesp-FGFRdn p=0.103, n=57). Scale bars = 10μm.

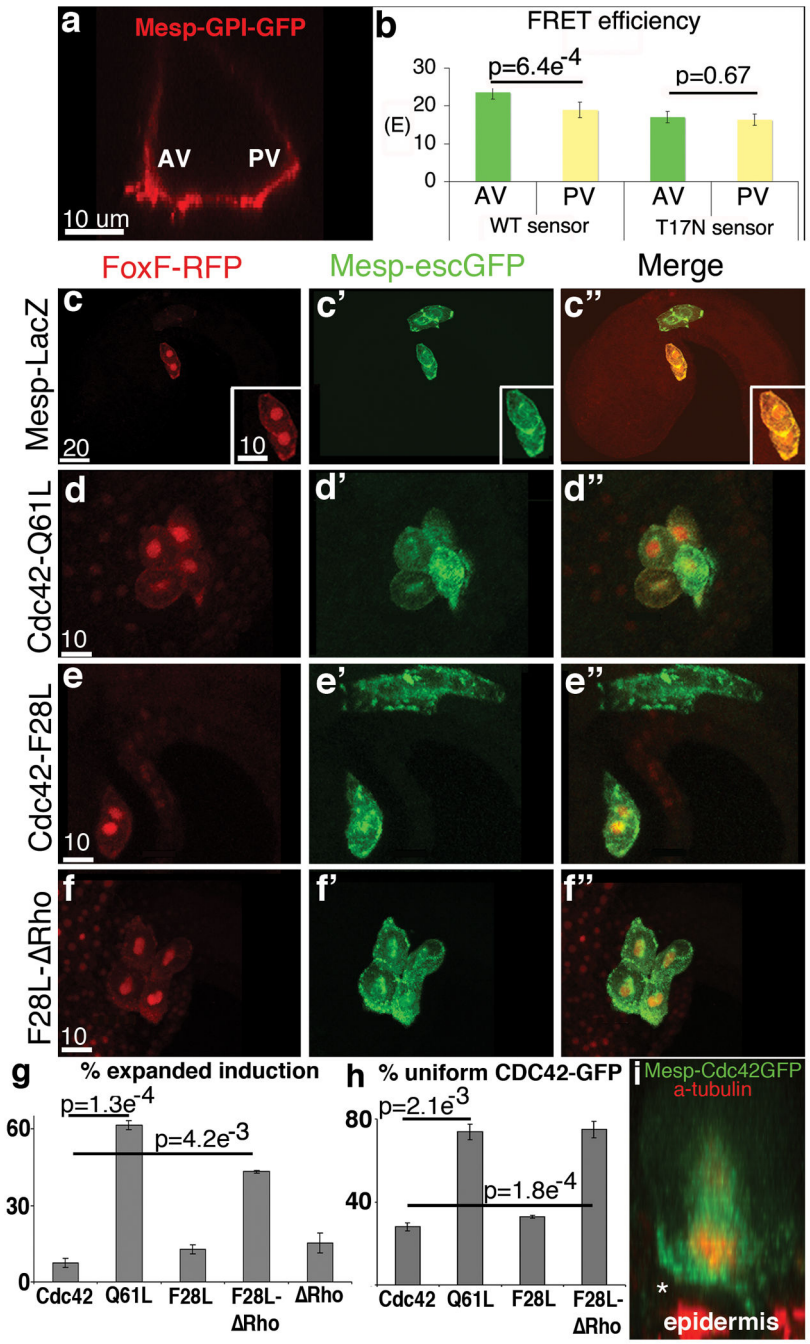

Figure 3. Localized CDC42 activity is required for differential induction

(**a**) Lateral optical section of a stage 14 GPI-GFP labeled founder cell illustrating the anterior-ventral (AV) and posterior-ventral (PV) regions used to generate FRET data. (**b**) FRET data, n=30 for WT sensor and n=26 for T17N, the inactive T17N probe serves as a negative control. (**c-f**) Representative results from induction assays, fluorescent reporters and transgenic backgrounds as indicated above and to the left respectively. Red channel in (**c″**) was amplified to better visualize the embryo. (**g-h**) Quantitative data showing % of transgenic embryos displaying; (**g**) loss of localized induction, n=375 for Cdc42, n=466 for

Q61L, n=461 for F28L, n=240 for F28L-ΔRho, and n= 250 for ΔRho and; (**h**) loss of polarized CDC42-GFP enrichment along the heart progenitor/ventral membrane, n=31 for Cdc42. n=31 for Q61L, n=25 for F28L, n=30 for F28L-ΔRho. (**i**) Lateral projection of dividing founder cell displaying enrichment of CDC42-GFP (green) along the presumptive heart progenitor membrane (asterisk). Scale bars in um as indicated.

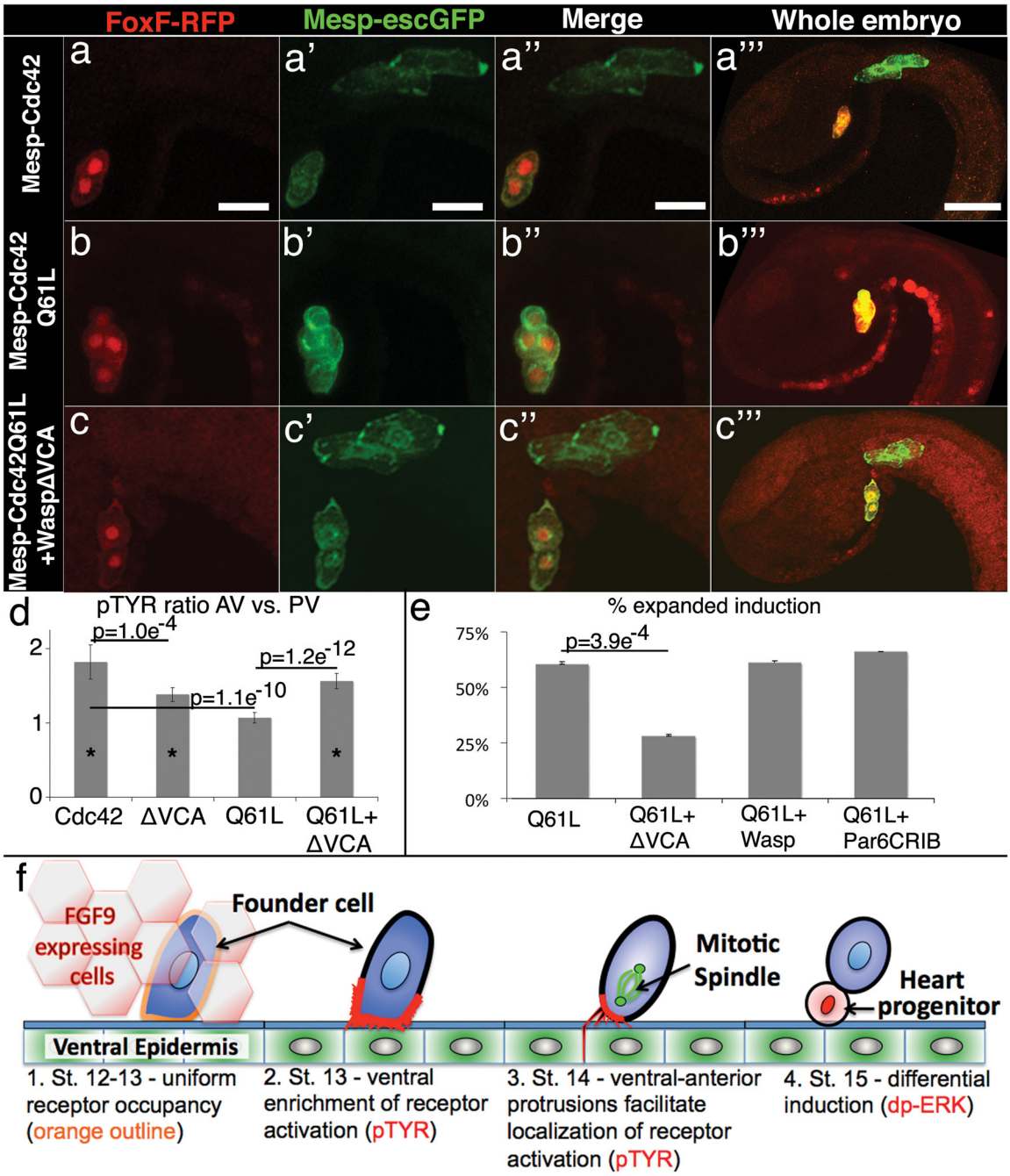

Figure 4. Cytoskeletal polarity directs differential induction

(**a-c**) Representative results from induction assays, reporters and transgenic backgrounds as indicated above and to the left respectively, scale bar = 20μm, in (**a‴-c‴**) the red channel has been amplified to better visualize the whole embryo, scale bar = 40μm. (**d**) pTyr ratio comparing AV to PV membranes, n=25 for cdc42, n=29 for WaspΔVCA, n=28 for Q61L and n=33 for Q61L+WaspΔVCA, asterisks indicates a significant difference ($p<0.005$) in the AV vs. PV measurements for that sample set. (**e**) Quantitative data for induction assays showing % of transgenic embryos with expanded induction, n=374 for Q61L, n=266 for

Q61L+WaspΔVCA, n=178 for Q61L+Wasp and n=307 for Q61L+ParCRIB; QL vs. QL +Wasp, p = 0.53, QL vs. QL+Par6CRIB, p = 0.81. (**f**) Four step model for differential specification of the heart progenitor lineage. 1. Ungraded exposure to growth factor leads to uniform receptor occupancy. 2. Receptor activation is enriched along the ventral membrane in association with enhanced protrusive activity. 3. As founder cells enter mitosis, localized invasive protrusions facilitate restriction of receptor activation to the ventral/anterior membrane. 4. Following division, Map Kinase pathway activation (nuclear dp-ERK) is restricted to the ventral daughter leading to differential expression of heart progenitor genes. See Supplemental Discussion for a more thorough explication of this model.